Open access • Journal Article • DOI:10.1109/TAP.2012.2207081

Chipless RFID Tag Using Multiple Microstrip Open Stub Resonators

— Source link

C. M. Nijas, R. Dinesh, U. Deepak, A. Rasheed ...+3 more authors

Institutions: Cochin University of Science and Technology

Published on: 03 Jul 2012 - IEEE Transactions on Antennas and Propagation (IEEE)

Topics: Chipless RFID and Microstrip

[9] E. Marcatili, "Dielectric rectangular wave guide and directional coupler for integrated optics," *Bell Syst. Tech. J.*, vol. 48, pp. 2071–2102, 1969.
[10] A. Petosa, *Dielectric Resonator Antenna Handbook*. Norwood, MA: Artech House, 2007.
[11] K. M. Luk and K. W. Leung, *Dielectric Resonator Antennas*. London, U.K.: Research Studies Press, 2003.
[12] G. Junker, A. Kishk, A. Glisson, and D. Kajfez, "Effect of fabrication imperfections for ground-plane-backed dielectric-resonator antennas," *IEEE, Antennas Propag. Mag.*, vol. 37, pp. 40–47, Feb. 1995.
[13] S. Shum and K. Luk, "Characteristics of dielectric ring resonator antenna with an air gap," *Electron. Lett.*, vol. 30, pp. 277–278, Feb. 1994.

Chipless RFID Tag Using Multiple Microstrip Open Stub Resonators

C. M. Nijas, R. Dinesh, U. Deepak, Abdul Rasheed, S. Mridula, K. Vasudevan, and P. Mohanan

***Abstract*—A novel compact RFID tag employing open stubs in a microstrip transmission line is proposed. The prototype of the tag is fabricated on a substrate of dielectric constant 4.4 and loss tangent 0.0018. The tag consists of microstrip open stub resonators and cross polarized transmitting and receiving disc monopole antennas. A prototype of 8 bit data encoded tag is demonstrated in this communication. Method for enhancing the performance of the RFID tag is also proposed. Magnitude or group delay response can be used to decode the tag informations.**

***Index Terms*—Chipless RFID tag, cross polarization, group delay, microstrip open stub, UWB antenna.**

I. Introduction

Radio frequency identification (RFID) can be conveniently employed to replace the barcode in the area of contactless data capturing. RFID doesn't require a face to face communication between data carrying device like transponder/RFID tag and interrogator/RFID reader. The RFID tag can be hidden inside the items and ensure more security and flexibility. The cost of the RFID tags with small chip is higher compared to barcode due to presence of application specific integrated circuit (ASIC) chip. Different RFID technologies are used for different applications. Some applications require short-range (up to 1.5 m) low-cost tags (luggage tagging), while others require long-range (over 20 m) and more reliable/robust tags (expensive equipment tagging or vehicle tagging).

RFID researchers are now focusing in the area of chipless RFID tags, in which bits are encoded in the frequency spectrum, and seem to be a promising solution for low-cost item tagging. Commercially available chipless RFID tags are developed by RFSAW and it is based on the surface acoustic waves (SAWs) [1]. These tags are not fully printable because of the piezoelectric components embedded in it. Fully printable chipless RFID based on group delay encoding [2], [3] and multi resonators [4] have been reported. Group delay based tag requires very large area for more number of bits. On the other hand, the power difference between the presence and absence of a bit is of the order of 1 dB in the case of multi resonator based RFID. This makes it very difficult for faithful identification.

Manuscript received February 07, 2012; revised April 12, 2012; accepted May 04, 2012. Date of publication July 03, 2012; date of current version August 30, 2012. This work was supported in part by the Department of Science and Technology (DST), Government of India and University Grants Commission (UGC), Government of India.

C. M. Nijas, R. Dinesh, U. Deepak, A. Rasheed, K. Vasudevan and P. Mohanan are with the Centre for Research in ElectroMagnetics and Antennas (CREMA), Department of Electronics, Cochin University of Science and Technology, Cochin-22, Kerala, India (e-mail: drmohan@gmail.com).
S. Mridula is with the School of Engineering, Cochin University of Science and Technology, Cochin-22, Kerala, India.

Color versions of one or more of the figures in this communication are available online at http://ieeexplore.ieee.org.
Digital Object Identifier 10.1109/TAP.2012.2207081

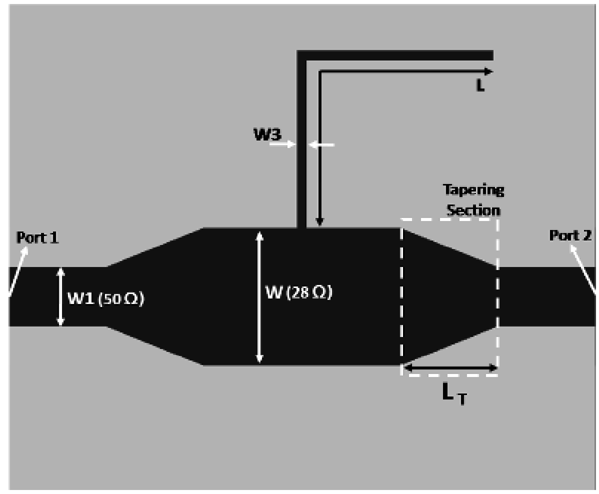

Fig. 1. Transmission line with quarter wave open stub resonator $W1 = 3$ mm, $W3 = 0.5$ mm, $W = 7$ mm $L_T = 12$ mm and $L = 18$ mm.

A chipless RFID tag with microstrip open resonators and cross polarized disc monopole antennas is discussed in this communication. The proposed tag is very compact and can be easily decoded due to the large difference between reflected power level corresponding to the presence and absence of a bit. Compared to [2], [4], [5], this tag offers a difference of 5 dB in magnitude and 6 ns in group delay and hence can be easily decoded.

II. Tag Design

The evolution of tag from a simple transmission line is demonstrated here. A microstrip transmission line of 50 Ω is fabricated on a substrate of dielectric constant 4.4 and loss tangent 0.0018. A $\lambda_g/4$ open circuited stub with appropriate end correction [6] is connected at the centre of the transmission line, where λ_g is the guided wavelength at the operating frequency. The basic structure of the tag incorporating an open ended microstrip stub is shown in Fig. 1. It is noted that there is a band notch centred at 2.35 GHz when an open circuited stub of length 18 mm and width 0.5 mm is connected to the microstrip transmission line. This property of the stub is effectively utilized for the development of the tag. Simulation studies of a single stub microstrip transmission line for different line parameters using Ansoft HFSS are shown in Table I. From Table I.a it is found that when the transmission line impedance is 50 Ω ($W = 3$ mm), the system offers a fractional band width (FBW) of 30.05%. The FBW is estimated using, $\mathrm{FBW} = \Delta f/f_0 * 100\%$, where Δf is the 3 dB S21 band width and f_0 is the notch frequency. The aim is to reduce the FBW to get the narrowest possible resonance at the desired frequency. However, when the transmission line impedance is about 28 Ω ($W = 7$ mm), optimum FBW (12.57%) is achieved. It is noted that further decrease in the impedance of the transmission line distorts the S_{21} characteristics. So this impedance is selected for further analysis. From Table I.b it is again found that when the width of the $\lambda_g/4$ stub (W3) is decreasing,

TABLE I
PARAMETRIC STUDY FOR THE OPTIMIZATION OF RFID TAG

Table 1.a. L1 = 18 mm, W3 = 0.5mm			**Table. 1. b L1 = 18 mm, W = 3mm**		
W (mm)	**F_0 (GHz)**	**FBW (%)**	**W3 (mm)**	**F_0 (GHz)**	**FBW (%)**
2	**2.37**	**39.42**	**0.3**	**2.33**	**27.27**
3	**2.35**	**30.05**	**0.5**	**2.35**	**30.05**
4	**2.32**	**23.50**	**0.7**	**2.36**	**33.69**
5	**2.31**	**17.90**	**0.9**	**2.38**	**37.21**
6	**2.30**	**15.11**	**1.1**	**2.41**	**39.48**
7	**2.29**	**12.57**	**1.3**	**2.44**	**40.08**
8	**2.27**	**9.21**	**1.5**	**2.47**	**44.45**

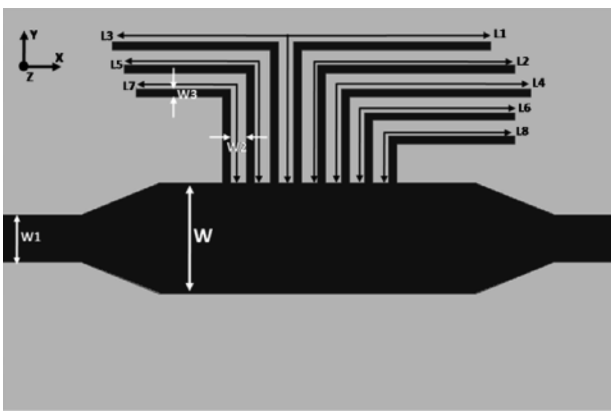

(a)

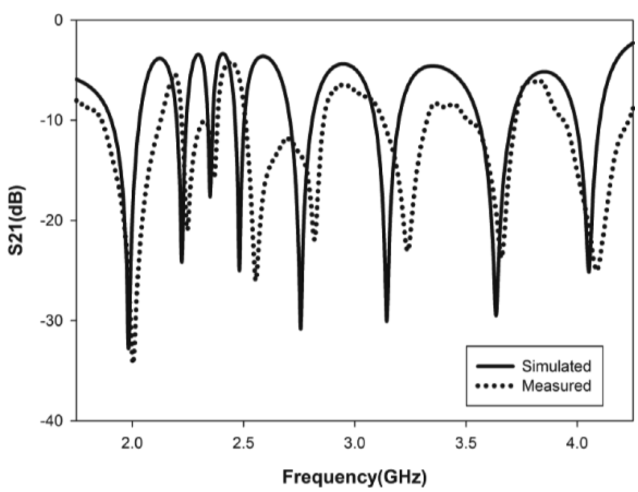

(b)

Fig. 2. (a) Proposed 8 bit open stub RFID tag, where $W = 7$ mm, $W1 = 3$ mm, $W2 = 1$ mm, $W3 = 0.5$ mm, $L1 = 21$ mm, $L2 = 19.5$ mm, $L3 = 19$ mm, $L4 = 17.5$ mm, $L5 = 15.25$ mm, $L6 = 13.5$ mm, $L7 = 11.5$ mm and $L8 = 10.5$ mm. (b) Frequency response of the proposed 8 bit tag [1111 1111] shown in Fig. 2(a).

FBW of the resonator is also decreasing. Due to the fabrication limitation, the width W3 is taken as 0.5 mm in the present study. It is also observed that there is a small frequency shift with the width of the stub. This may be due to the increased inductance of the stub for small

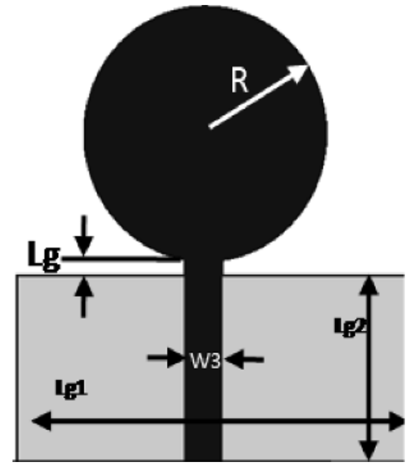

(a)

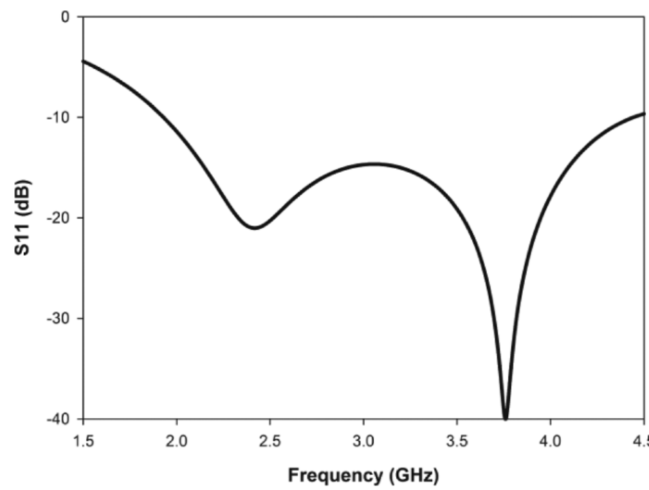

(b)

Fig. 3. (a) Disc monopole antenna $R = 15$ mm, $W3 = 3$ mm, $Lg = 0.6$ mm, $Lg1 = 40$ mm and $Lg2 = 20$ mm. (b) Simulated reflection characteristics of disc monopole antenna described in (a).

width [7]. Similarly the small shift in the resonance with the width of the transmission line may be due to the change in effective capacitance of the line with width. To reduce the effect of impedance mismatch between 50 Ω and 28 Ω in the microstrip transmission line, an impedance transformer section (tapering section) is also included [8]. Length of this tapering section (L_T) is equal to 0.25 $\lambda_{d,}$ where λ_d is the wavelength in the substrate corresponding to lowest frequency of operation.

From the above knowledge an 8 bit RFID tag is designed as illustrated in the Fig. 2(a). The overall dimension of the tag is 30 × 25 × 1.6 mm^3. Each resonator is independently resonating at its quarter wavelength frequency ($\lambda_g/4$). To avoid the mutual coupling between the two resonators they are kept 1 mm apart. Experiments are conducted using PNA E8362B. Fig. 2(b) shows the measured and simulated frequency response of the 8 bit RFID tag. The simulated results show very good agreement with the measured values.

For a complete chipless RFID tag, disc monopole UWB antennas have been used as the receiving and retransmitting antenna on the RFID tag [9]. Fig. 3(a) shows the geometry of the monopole antenna, along with the design parameters. The simulated response of the antenna in the operating band of the tag is shown in Fig. 3(b). This confirms that the antenna is operating in the range of 1.9 GHz to 4.5 GHz.

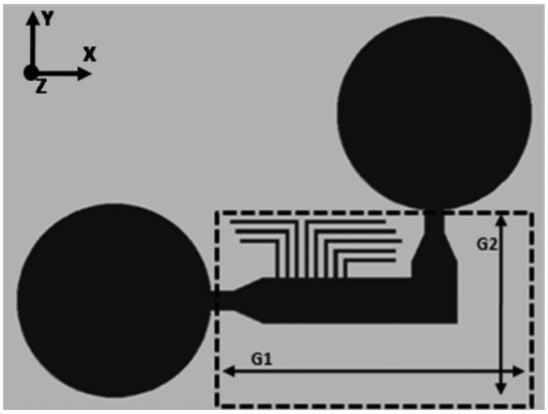

Fig. 4. 8 bit RFID Tag with disc monopole antenna, $G1 = 50$ mm, $G2 = 30$ mm, dotted line showing the ground at the backside of the substrate ($\varepsilon_r = 4.4$, $\tan\delta = .0018$ and height $= 1.6$ mm).

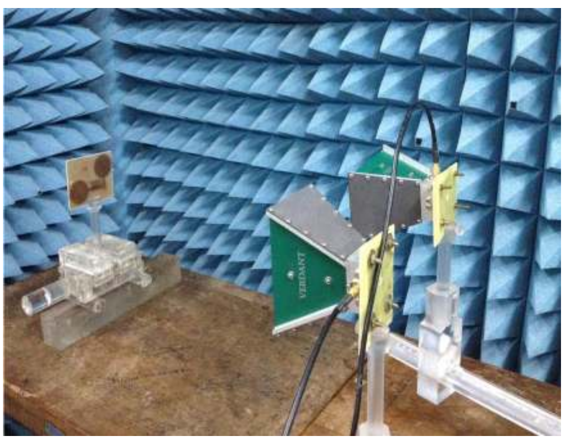

Fig. 5. Measurement set up inside the anechoic chamber.

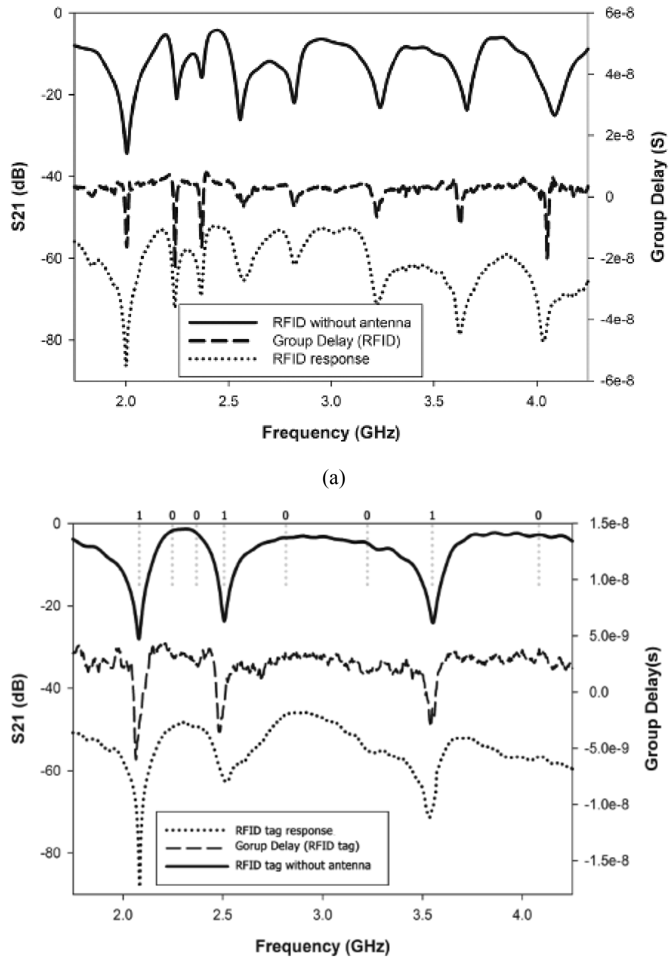

(a)

(b)

Fig. 6. (a) Measured response of RFID tag (1111 1111). (b) Measured response of RFID tag (1001 0010).

III. Results and Discussion

The receiving and retransmitting antennas are connected in such a way that they are orthogonally polarized [4]. The backscattered signal from the retransmitting antenna has been used for the encoding purpose. Eight independent resonators are added to the transmission line of characteristic impedance 28 Ω as shown in the Fig. 4. The individual resonators are operating at different frequencies (2.08 GHz, 2.23 GHz, 2.36 GHz, 2.56 GHz, 2.81 GHz, 3.21 GHz, 3.61 GHz and 4.03 GHz corresponding to the bit pattern 1111 1111). The overall dimension of the RFID tag is $80 \times 60 \times 1.6\ \mathrm{mm}^3$. Two medium gain (8 dBi) horn antennas are used at the reader side for transmitting and receiving signals from the RFID tag. Back scattered signal from the retransmitting antenna is very weak to identify the response of the tag. Hence, calibration procedure mentioned in [10] was followed for the measurement.

The measurement set up inside the anechoic chamber is shown in Fig. 5. The tag is placed about 40 cm away from horn antennas. Magnitude and Group Delay studies were carried out using PNA E8362B. Identification of each bit is very clear from magnitude and group delay measurements. Typical response of the RFID tag for 1111 1111 and 1001 0010 bits are shown in Fig. 6(a) and (b) respectively. From Fig. 6(a), it is clear that there is a small shift in the resonant frequency due to mutual coupling effect between the resonators. RFID tag without antenna, with the network analyzer ports connected directly as in Fig. 1 is also shown in Fig. 6 for comparison. The band notches are well defined and for the worst case the magnitude of the dip is better than 5 dB. The measured group delay response of the RFID tag is also shown in Fig. 6. It is noted that group delay of a narrow band notch resonator at resonance is negative [11] and can be easily detected. From the figure, it is well understood that the magnitude and group delay can be conveniently used for reading the tag.

IV. Conclusion

A novel RFID tag with multiple open stub resonators is proposed in this communication. The tag is very compact and enables to encode data in magnitude as well as in group delay. Replacing the disc monopole antenna with compact UWB antenna can make RFID tag even smaller. The method introduced in this communication can be effectively implemented using low cost substrate materials which in turn reduce the overall cost.

Acknowledgment

The authors acknowledge Dr. R. Ratheesh, Scientist, C-MET, Trichur for providing research support.

References

[1] C. S. Hartmann, "A global SAW ID tag with large data capacity," in *Proc. IEEE Ultrason. Symp.*, Munich, Germany, Oct. 2002, vol. 1, pp. 65–69.

[2] R. Nair, E. Perret, and S. Tedjini, "Chipless RFID based on group delay encoding," presented at the IEEE Int. Conf. on RFID-Technologies and Applications, Sitges, Spain, Sep. 15–16, 2011.

[3] S. Gupta, B. Nikfal, and C. Caloz, "Chipless RFID system based on group delay engineered dispersive delay structures," *IEEE Antennas Propag. Lett.*, vol. 10, pp. 1366–1368, 2011.

[4] S. Preradovic, I. Balbin, N. C. Karmakar, and G. F. Swiegers, "Multiresonator-Based chipless RFID system for low-cost item tracking," *IEEE Trans. Microw. Theory Tech.*, vol. 57, no. 5, May 2009.
[5] V. Deepu, A. Vena, E. Perret, and S. Tedjini, "New RF identification technology for secure applications," presented at the IEEE Int. Conf. on RFID-Technology and Applications, Guangzhou, China, Jun. 17–19, 2010.
[6] M. Kirsching, R. H. Jansen, and N. H. L. Koster, "Accurate model for open end effect of microstrip lines," *Electron. Lett.*, pp. 123–125, Feb. 1981.
[7] J.-S. Hong and M. J. Lancaster, *Microstrip Filters for RF/Microwave Applications*. New York: Wiley-Interscience, 2001, pp. 112–120.
[8] P. A. Rizzi, *Microwave Engineering Passive Circuits*. New York: Pearson, 2007, pp. 152–54.
[9] S. Preradovic, I. Balbin, N. C. Karmakar, and G. Swiegers, "A novel chipless RFID system based on planar multiresonators for barcode replacement," in *Proc. IEEE Int. Conf. RFID*, Las Vegas, Apr. 16–17, 2008, pp. 289–296.
[10] A. Vena, E. Perret, and S. Tedjini, "RFID chipless tag based on multiple phase shifters," in *Proc. IEEE Int. Microwave Symp. Digest*, Jun. 5–10, 2011, pp. 1–4.
[11] Group Delay Explanations and Applications Applied Radio Labs [Online]. Available: www.radiolab.com.au

Millimeter-Wave Integrated Pyramidal Horn Antenna Made of Multilayer Printed Circuit Board (PCB) Process

Nasser Ghassemi and Ke Wu

***Abstract*—Due to the low atmospheric absorption over W-band, numerous applications are expected, which should be developed at low cost. Short wavelength makes the dimension of antennas in this frequency range small, which usually requires sophisticated and expensive fabrication process. This communication presents a class of integrated wideband pyramidal horn antennas which can be made of low-cost multilayered printed circuit board (PCB) process. The proposed horn antenna radiates along the broadside to the substrate and uses substrate integrated waveguide (SIW) as its feeder. Transverse slot on the top metallic surface at the end of SIW is deployed to drive the horn antenna. Metalized via holes are used to synthesize the horn walls. The opening of the horn antenna is discretely flared from the bottom to the top layer. Measured bandwidth of the antenna is 35 GHz (70–105 GHz) while a relatively constant gain of 10 $\pm$ 1 dB is obtained over most of the bandwidth.**

***Index Terms*—E band, integrated horn antenna, multilayered PCB, substrate integrated waveguide (SIW), W-band.**

I. INTRODUCTION

According to the well-known frequency-dependent atmospheric absorption curve [1], the atmospheric attenuation decreases significantly over the W-band frequency range, leading to a propagation window. With the allocation to higher millimeter-wave frequencies, wireless communication systems can operate in a much less crowded part of the electromagnetic spectrum. This means more bandwidth will be available for transmitting large-volume information data. Increasing frequency also increases the angular resolution, which is valuable in the development of radar and imaging systems [2]. This gives the aptitude of a long range Gigabyte data transmission at the rang of several kilometers (in normal weather condition) using a point-to-point wireless communication link [3], and a high resolution long range imaging system which has such applications as high resolution radars, sensors, and imaging systems [4], [5]. All these systems require low-cost and small footprint antenna which is one of the important parts in the design of such systems.

At millimeter-waves, microstrip feed lines are known to suffer from serious transmission losses [6]. Although several microstrip array antennas have been studied for millimeter-wave radar and communication systems, the increasing of frequency and gain is accompanied with the decreasing of radiation efficiency because of the inherent losses on the microstrip feeding network. Waveguide has many applications because of its high efficiency with the smallest conductor losses [7]. However, they suffer from their bulky structures, and their prohibitive cost especially at millimeter wave frequencies. Substrate integrated waveguide (SIW) was proposed to overcome the disadvantages of the above-mentioned conventional guided-wave techniques [8]. SIW consists of arrays of metallic via holes created in a planar substrate. Low-cost standard PCB process can be used to fabricate SIW structures. SIW can easily be connected to coplanar waveguide (CPW) [9] utilizing a planar wideband transition. It offers the integration of millimeter-wave planar circuits and SIW-based antenna on the basis of a low cost PCB process.

With reference to antenna techniques, horn structure has found a large number of applications thanks to its simplicity, wide bandwidth, and high gain. The fundamental problem of this structure lies in its integration problem and cost issue. Several horn antennas over millimeter-wave and sub-millimeter-wave frequency range were presented [10]. As frequency increases, the dimension of the antenna becomes smaller due to the shorter wavelength. Usually, it may need a micromachining fabrication process which then increases the cost of the antenna [10]. Especially, fabricating a corrugated or stepped horn antenna [11]–[14] is expensive and difficult at such high frequencies. At high millimeter-wave frequencies, connecting the horn antenna to active microwave components is also very difficult. Certainly, it would increase the cost of the antenna and its related system. SIW-based H-plane horn antennas were presented in [15]–[18], which provide an alternative planar solution to classical horn techniques. Although these structures are low-cost and can easily be interfaced with CPW or microstrip lines, their bandwidth is relatively narrow and they radiates in parallel to the substrate which is not desirable for many practical applications.

This communication presents a novel wideband integrated SIW-fed horn antenna in synthesized planar form which radiates along the broadside to the substrate. The proposed antenna is easy to integrate with CPW line. A low-cost multilayer PCB process is used to fabricate the antenna on Rogers substrate. Measured bandwidth of the antenna is 40% (70–105 GHz) and measured gain of the antenna is about 9.5 dB over the most of the antenna bandwidth. Compared to the other SIW-fed integrated horn antennas [15]–[18], the proposed structure presents much wider bandwidth and it has broadside-to-the-substrate radiation pattern, which is stable within the bandwidth of interest. Note that the antenna thickness in connection with the number of layer is increased.

II. ANTENNA STRUCTURE AND DESIGN

Fig. 1 shows the configuration of a waveguide-based horn antenna and its waveguide feed. The goal of this work is integrating this waveguide-based horn antenna made in a low cost multilayer structure. The

Manuscript received July 23, 2011; revised January 04, 2012; accepted May 03, 2012. Date of publication July 10, 2012; date of current version August 30, 2012.

The authors are with the Poly-Grames Research Center and Center for Radiofrequency Electronics Research of Quebec (CREER), Department of Electrical Engineering, Ecole Polytechnique (University of Montreal), Montreal, QC H3V 1A2 Canada (e-mail: nasser.ghassemi@polymtl.ca; ke.wu@ieee.org).

Color versions of one or more of the figures in this communication are available online at http://ieeexplore.ieee.org.

Digital Object Identifier 10.1109/TAP.2012.2207050